Electrical resistivity imaging for the characterization of the Montaguto landslide (southern Italy)

Jessica Bellanova[a] Giuseppe Calamita[a] Alessandro Giocoli[b] Raffaele Luongo[a] Maria Macchiato[c] Angela Perrone[a] Sebastian Uhlemann[d1] Sabatino Piscitelli[a]

Abstract

Electrical Resistivity Tomography surveys were carried out for the characterization of the Montaguto earth-flow, located in the southern Apennines chain (Campania Region, southern Italy). The earth-flow investigated is one of the largest and most complex landslides in Europe with a length of 3.1×10^3 m, a width ranging between 45 and 420 m and an area of about 6.6×10^5 m^2. In the spring of 2010, a large reactivation of the earth-flow heavily damaged some strategic infrastructures. In order to mitigate the effects of the mass movement, considerable efforts were carried out by the Italian National Civil Protection Department (DPC) to tackle the emergency. The aim of the study was to contribute to a more accurate geometric reconstruction of the landslide body and to improve the knowledge of the geological setting. Due to the lithological characteristic of the outcropping lithotypes, i.e. Faeto Flysch (calcarenite, clay and marl) and Villamaina Unit (sand and silty clay), the electrical resistivity contrasts were not very pronounced. However, the high-resolution of the electrical tomographies was the key to observe the presence of both lateral and vertical discontinuities that were associated with lithological boundaries, structural features and sliding surfaces. The results of the geoelectrical surveys could be considered for planning additional and more appropriate actions aimed at the stabilization of different portions of the Montaguto landslide.

Keywords: Electrical resistivity tomography, Landslide, Earth-flow, Montaguto, Southern Italy

1. Introduction

The Montaguto landslide, located in southern Apennines chain (Campania Region, southern Italy), is one of the largest and most complex earth-flows in Europe (Fig. 1). It was active for almost 60 years, with records dating back to 1954. Long periods of relatively slow movements and shorter periods of relatively rapid movements have occurred periodically during the earth-flow activity (Guerriero et al., 2013).

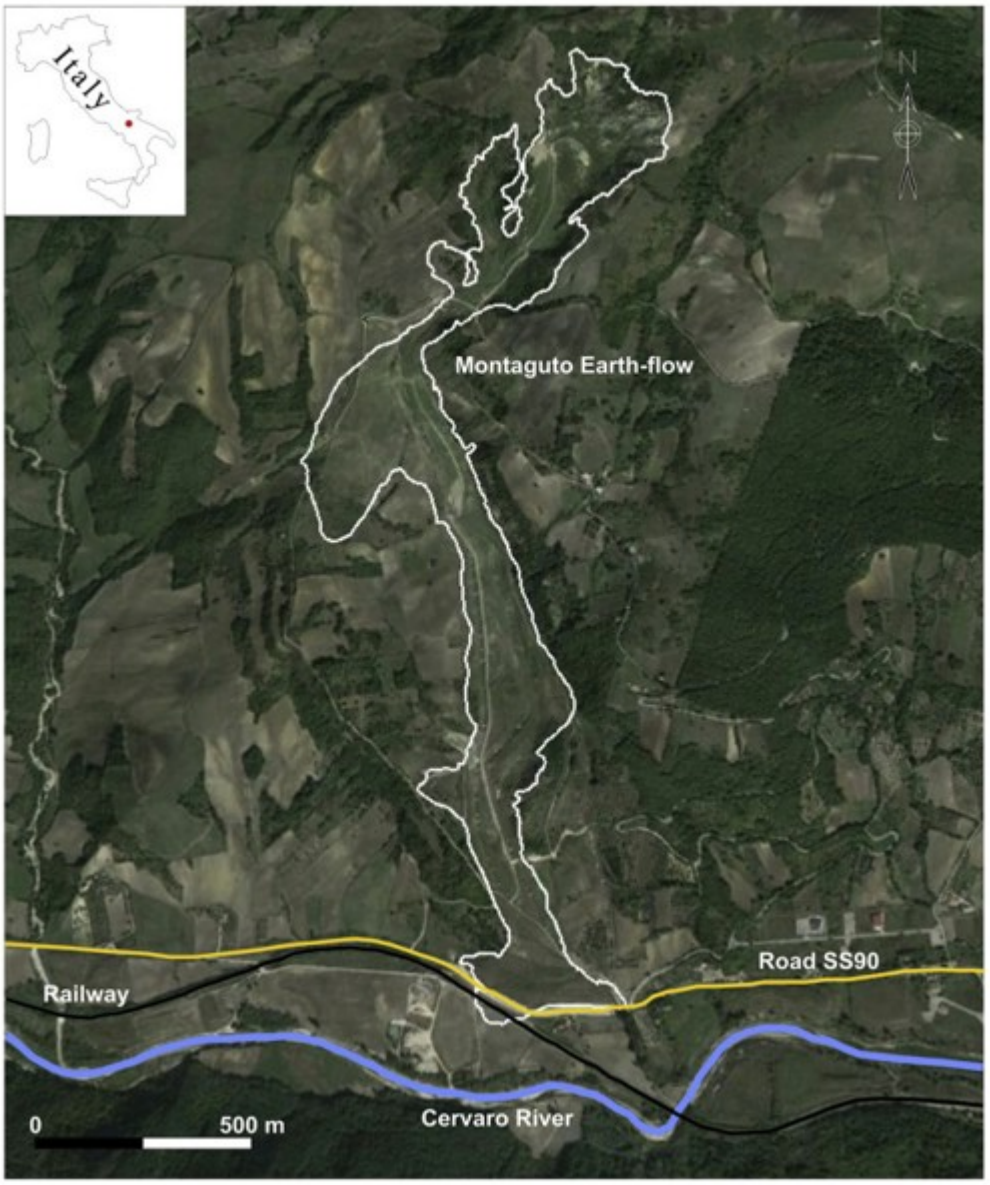

Fig. 1. Location of the Montaguto earth-flow, southern Apennines (Campania Region, southern Italy). White line: landslide boundary. Black line: railway. Yellow line: road SS90. Blue line: Cervaro River (Image from Google Earth - acquisition date: 2014).

On 26th April 2006 a large earth-flow remobilization covered the SS90 National Road with an estimated volume of $6 \times 10^6\,m^3$ (Guerriero et al., 2013). Four years later, in the spring of 2010, a reactivation of the earth-flow reached the Cervaro River valley obstructing and heavily damaging the strategic National Railway infrastructure that connects the towns of Naples and Bari, and the SS90 National Road, which connects Campania and Puglia Regions (Ventura et al., 2011; Giordan et al., 2013). Considerable efforts were carried out by the Italian National Civil Protection Department (DPC) to tackle the emergency. In order to mitigate the effects of the mass movement, a series of interventions have been conducted since then, i.e.

design and construction of an artificial drainage system, removal of slide material from the toe, etc. (Giordan et al., 2013; Lollino et al., 2014). Despite the achieved deceleration of the earth-flow, there was a need to implement further coordinated actions to ensure secure conditions for the railway and road infrastructures. To realize a well structured and comprehensive intervention plan further relevant geological, geotechnical and geophysical information (e.g., mechanical characteristics of the material, geometry of the body, etc.) was required.

This paper reports on the results of an Electrical Resistivity Tomography (ERT) survey carried out on the upper and central part of the landslide area to obtain geophysical information on the materials involved in the movement, to improve the knowledge about the geological setting and to characterize the geometry of this portion of the landslide. In particular, the survey was focused on the landslide sector between about 600 and 520 m a.s.l., where a trend of continuous movement was evident despite the drainage interventions (Ferrigno et al., 2017). In contrast to other sectors of the landslide body, this state of activity required a detailed analysis of the monitoring activities, as highlighted by other authors (Lollino et al., 2013; Lollino et al., 2014).

2. Geological, geomorphological and climatic settings

The area affected by the Montaguto earth-flow is located in a region known as “Daunia Apennines” in the eastern part of the southern Apennines. The Daunia Apennines belong to the highly deformed transition area between the frontal thrusts of the Apennine chain and the western part of the foredeep (Crostella and Vezzani, 1964; Dazzaro et al., 1988). In this area, the lithological units are characterized by the presence of flysch units of Miocene age, rich in clay component, which are intensely deformed as a result of the tectonic history of the Apennines (Amore et al., 1998; Di Nocera et al., 2011) and prone to landsliding. Usually, the activity of landslides is characterized by seasonal remobilizations of slope movements, typically due to rainfall events. The study area shows outcrops of the Faeto Flysch (FF), belonging to the Daunia Unit (Crostella and Vezzani, 1964), the Villamaina Unit (FV) (Di Nocera and Torre, 1987; Pescatore et al., 1996), colluvial deposit (d) and alluvial sediments (a). The Faeto Flysch and the unconformable overlying Villamaina Unit are outcropping in the upper part and in the middle-lower sector of the landslide, respectively; the alluvial sediments are present in the Cervaro River valley (Guerriero et al., 2014) (Fig. 2).

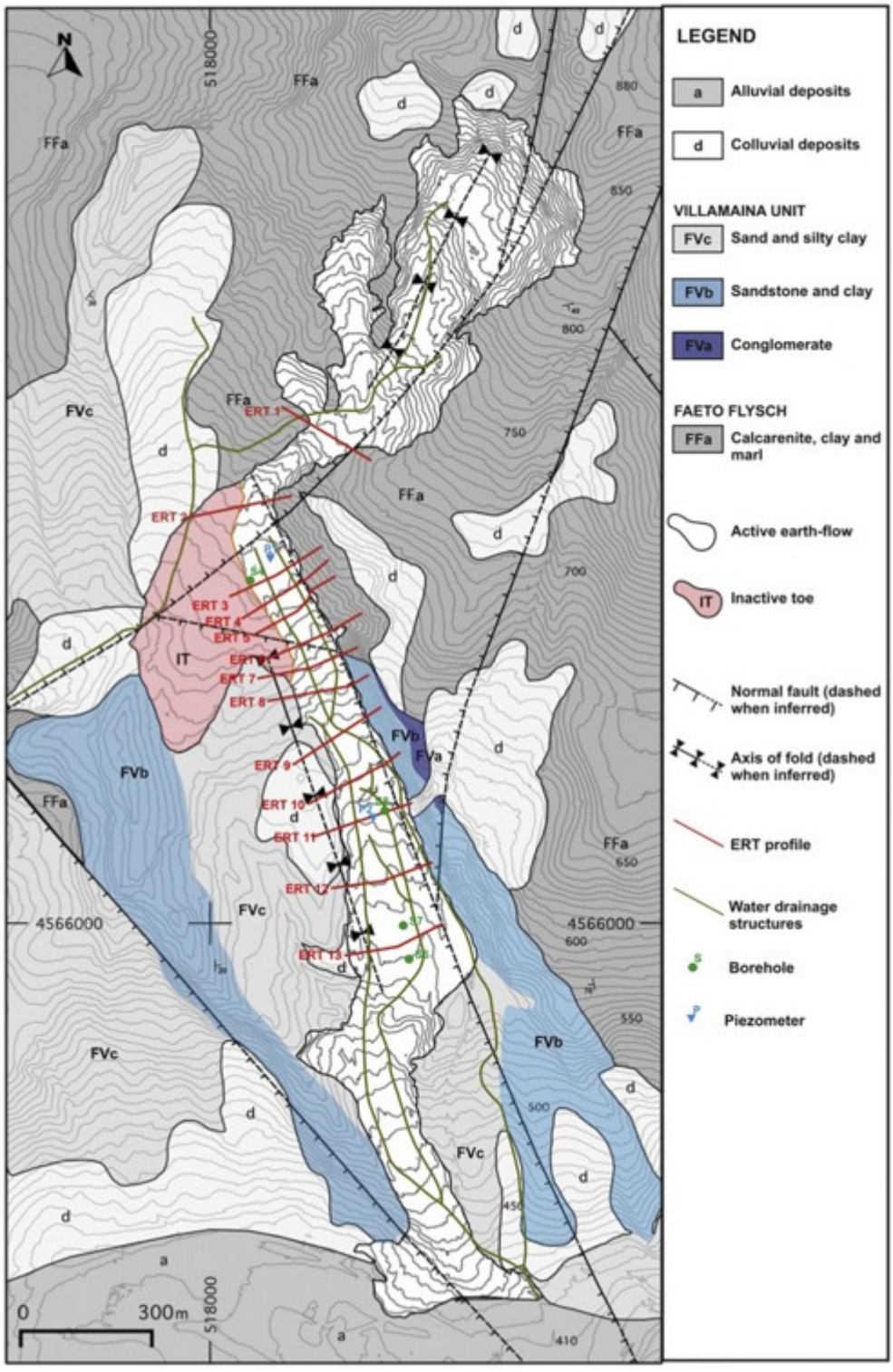

Fig. 2. Geological map of the Montaguto earth-flow. Legend: colluvial deposits (d); alluvial deposits (a); Villamaina Unit (FVa: conglomerate; FVb: sandstone and clay; FVc: sand and silty clay); Faeto Flysch(FFa: calcarenite, clay and marl); line with hachures: normal fault (dashed when inferred); line with triangles: axis of fold structure. The white area indicates the active earth-flow. The pink area indicates the inactive toe of the old landslide (IT). Red lines: ERT profiles. Green line: water drainage

structures. Green dot: borehole. Blue triangle: piezometers. Coordinates in UTM 33 N are shown (modified from Guerriero et al., 2014).

The Faeto Flysch, aged from Langhian to Tortonian, is composed by basinal and shelf margin facies and consists of three lithofacies, which from the bottom upward are: a calcareous-clayey-marly succession (FFa), composed of calcarenite and clay, passing upwards to calcarenite, calcirudite and white marl; a calcareous-marly succession (FFb), represented by a dense alternation of calcarenite and marl, and a clayey-marly-calcareous succession (FFc) that consists of calcarenite, white marl and green clay (Santo and Senatore, 1988). The slope affected by the studied earth-flow is only characterized by outcrops of the basal member of the Faeto Flysch (FFa) (aged Burdigalian sup. - Langhian inf.), which locally has a prevalently calcareous-marly or clayey composition. The Villamaina Unit, Early Messinian in age, is made up of conglomerates (FVa), poorly cemented sandstones with a few clay beds (FVb) and, upwards, brownish-gray sands with silty claybeds (FVc) (Lollino et al., 2014).

The recent 2010 Montaguto landslide is characterized by a length of 3.1×10^3 m, a width ranging between 45 and 420 m, and an area of about 6.6×10^5 m^2 (~66 ha) (Ventura et al., 2011; Giordan et al., 2013). Previous studies (Guerriero et al., 2013; Lollino et al., 2014) estimated the volume of displaced material to be about 4×10^6 m^3 and the depth of the sliding surface to vary from about 5 m near the channel area to 20–30 m at the toe. As stated by Ventura et al. (2011), the depth of the water table roughly corresponds to the thickness of sliding materials with sag ponds occurring in the upper and central zone. The difference in altitude between the landslide head scarp, 830 m a.s.l., and the toe, 420 a.s.l., is about 410 m (Giordan et al., 2013). Between 1954 and 2010, velocities of most movements were reported to have ranged between 1 and 2 mm/month and 2–5 cm/day. A sharp increase was registered during the large mobilization in 2006 and 2010, where velocities change from 1 m/day to 1 m/h, as reported by Guerriero et al. (2013), or 5 m/day, as reported by Giordan et al. (2013).

As reported by other authors (Guerriero et al., 2014), long-term rain-gauge measurements (1921–2009) indicate cumulated annual precipitation varying between 200 and 1400 mm/y, with an average of 800 m/y. Rain-gauges were installed at five different sites about 10 km from Montaguto (Orsara di Puglia, Monteleone di Puglia, Savignano Irpino, Faeto, and Bovino) and recorded precipitation data between 1957 and 1987. Those data indicate July as the driest month of the year, with a mean of about 30 mm of cumulated rainfall, while November and December are the months with the highest precipitations, i.e. mean precipitation of 100 mm (Desiato et al., 2007). In October 2011, when the ERT data presented in this paper were acquired, the rain-gauges of Castelfranco in Misciano and Ariano Irpino2, both placed at about 10 km from the landslide, recorded only 50 mm of rainfall (Centro funzionale multirischi, Regione Campania).

3. The electrical resistivity tomography method

Landslides are complex geological phenomena characterized by an extremely large diversity in terms of area, volumes, speed and triggering mechanism (Cruden and Varnes, 1996; Guzzetti, 2006). A good designed strategy for landslide characterization requires a multidisciplinary approach ideally with the integration of data coming from different sources, such as ground-based, airborne and satellite-based sensors. Among the ground-based methods, the widely used direct techniques (e.g., boreholes, piezometers, inclinometers and laboratory tests) yield *true* parameters on the lithological, hydrological and geotechnical characteristics of landslide bodies. However, as these techniques can only provide information at specific points in the subsoil, the spatial delineation of subsurface features would require a high number of tests leading to a clear increase in costs. In situ geophysical techniques, however, permit non-invasive measurements of physical parameters directly or indirectly linked with the lithological, hydrological and geotechnical characteristics of the materials related to the movement (Perrone et al., 2014). Moreover, by providing information on bigger volumes of the subsoil, geophysical surveys overcome the point-scale feature of classic geotechnical and hydrological measurements (Calamita et al., 2017). Electrical Resistivity Tomography is one of the most widely used geophysical techniques for landslides characterization (McCann and Foster, 1990; Jongmans and Garambois, 2007; Niesner and Weidinger, 2008; Perrone et al., 2014). The ERT method provides an image of the distribution of the subsoil electrical resistivity, a geophysical parameter sensitive to the nature of material (particularly clay content), to the water content and its electrical conductivity, as well as to the rock weathering and fracturing. For these reasons, ERT has been applied to define the geological setting of subsoils, to reconstruct the geometries of landslide bodies (Hack, 2000; Perrone et al., 2004; Naudet et al., 2008, Chambers et al., 2011, Supper et al., 2013, Giocoli et al., 2015), to locate sliding surfaces and lateral boundaries (Gallipoli et al., 2000, Lapenna et al., 2003, Lapenna et al., 2005, Lebourg et al., 2005), and to evaluate the groundwater conditions (Lapenna et al., 2003, Perrone et al., 2006, Uhlemann et al., 2017).

Resistivity measurements are made by injecting a controlled electric current into the ground through two steel electrodes and measuring the potential drop at two other electrodes. An apparent resistivity value (ρ_a) is calculated taking into account the intensity of the injected current (I), the measured potential drop (V) and a geometric coefficient (k) related to the spatial electrode configuration, $\rho_a = k \cdot V/I$. Different electrode arrays, such as Wenner, Schlumberger, dipole-dipole, etc., can be used for ERT surveys. To obtain a subsurface image of the electrical resistivity, the measured apparent electrical resistivity data have to be inverted, by means of specific inversion software, to estimate the geological model parameters, i.e. the *true* electrical resistivity and the layer geometry (Sharma and Verma, 2015).

In this work, apparent electrical resistivity data were acquired through a multi-electrode system (48 electrodes) using a Syscal Junior (Iris

Instruments) resistivity meter connected to a multi-core cable. A constant spacing (a) of 5 m between adjacent electrodes was used and different array configurations (Wenner–Schlumberger and dipole–dipole) were adopted with different combinations of dipole length (1a, 2a and 3a) and number of depth levels “n” ($n \leq 6$). The investigation depth was about 40 m. Data noise was assessed by means of the stacking procedure (Robert et al., 2011). Five to ten stacked measurements of electrical resistivity were carried out for each point and the respective relative standard deviation (Dev parameter, also called Q-factor) was automatically estimated by the resistivity-meter. The values of resistivity characterized by a standard deviation >1% and all obvious outliers were removed. The apparent electrical resistivity data were inverted using the RES2DINV software (Loke, 2004) to obtain the 2D electrical resistivity images of the subsurface. The inversion routine is based on the smoothness-constrained least-squares inversion method implemented by using a quasi-Newton optimisation technique (Sasaki, 1992; Loke and Barker, 1996). The optimisation method adjusts the 2D electrical resistivity model trying to iteratively reduce the difference between the calculated and measured apparent resistivity values. Both least-square (L2) and robust (L1) norms were used. The former was preferred as it assumes smooth changes of the subsurface resistivity. The best results were obtained by means of the Wenner–Schlumberger (WS) array, which showed a higher signal-to-noise ratio, a greater investigation depth and a better sensitivity patterns to both horizontal and vertical changes in the subsurface resistivity (Loke, 2004).

All ERT profiles, each with a length of 235 m, were placed perpendicularly to the main axis of the channel area of the landslide (Fig. 2): two ERT profiles were carried out in the upper-zone of the channel area between 700 m and 620 m a.s.l., and eleven ERT profiles were realized in the central part of the channel area, along parallel profiles spaced 50–60 m apart. The main aim of this survey was to characterize the geometry of this portion of the landslide, to improve the knowledge about the geological setting and to indirectly test the effectiveness of the specifically installed drainage system. The latter could represent a very important information for the technicians of DPC, because this portion of landslide, despite the implemented drainage interventions (excavation, surface drainage, etc.), was characterized by a trend of continuous movement (Lollino et al., 2013, Lollino et al., 2014; Ferrigno et al., 2017).

4. Results

For all ERT profiles the range of the electrical resistivity values is limited, varying between 3 and >34 Ωm. Since the electrical resistivity of a rock is controlled by different factors (water content, porosity, clay content, etc.), there are generally wide ranges in electrical resistivity for any particular rock type and, accordingly, electrical resistivity values cannot be directly interpreted in terms of lithology. For these reasons, we used data from literature (Giocoli et al., 2008; Mucciarelli et al., 2009), geological surveys, exploratory boreholes, direct and indirect surveys (e.g. static cone-

penetration tests and shallow-seismic profiles in Guerriero et al., 2014) and direct resistivity measurements on outcrops to calibrate the ERT and to directly correlate electrical resistivity values with the lithostratigraphic characteristics. Thus, although the resistivity models are characterized by low to moderate resistivity contrasts, the following electrical resistivity ranges were assigned: $\rho > 12\,\Omega m$ to the prevalently calcareous-marly material of FFa, $\rho < 12\,\Omega m$ to the clayey deposit of FFa, $\rho > 12\,\Omega m$ to FVb and $\rho < 12\,\Omega m$ to FVc. In particular, the active landslide material is characterized by electrical resistivity values ranging between 6 and 20 Ωm, whereas the inactive earth-flow show about $\rho < 6–7\,\Omega m$.

Fig. 2 shows the profiles (red lines) along which ERT were carried out. The profiles cross (active and inactive) landslide material and terrains belonging to the FF and FV. Taking into account the low precipitation values recorded during October 2011 at nearby rain-gauges(see Section 2), the low electrical resistivity values can be explained by the lithological composition of the formations involved in the landslide.

Despite low resistivity contrasts, the ERT allowed us to define the geometry of active and inactive landslide bodies, to identify sub-vertical discontinuities, often corresponding with the lateral limits of the earth-flow, and to locate areas characterized by higher water content (Fig. 3, Fig. 4, Fig. 5, Fig. 6).

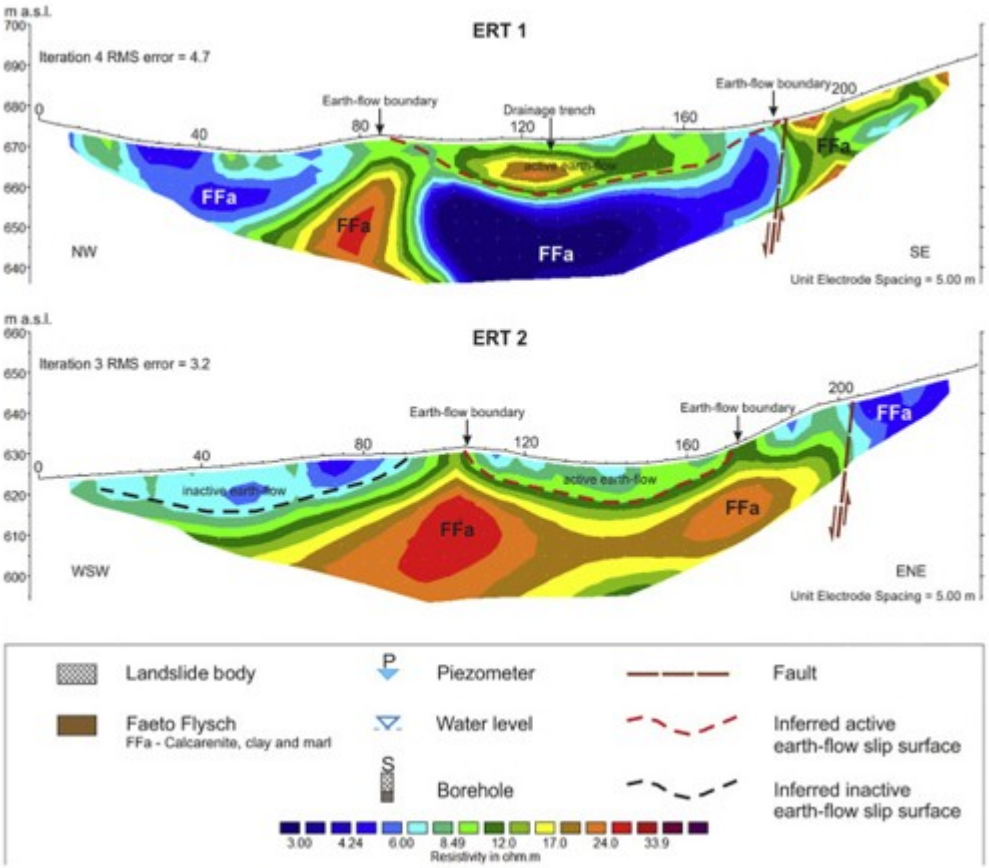

Fig. 3. Resistivity models of 1–2 ERT carried out in the upper zone of the channel area of the Montaguto landslide.

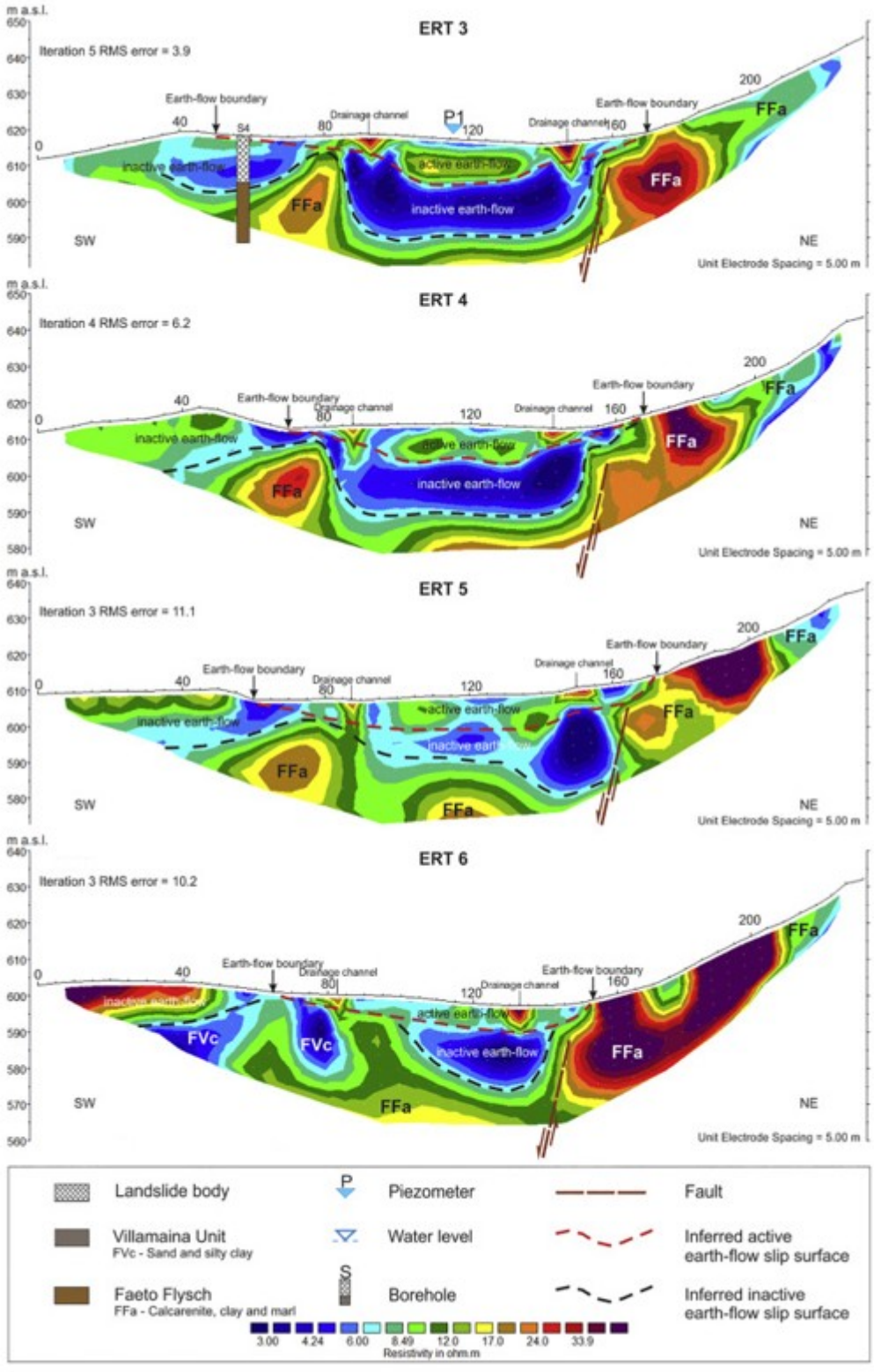

Fig. 4. Resistivity models of 3–6 ERT carried out in the central part of the channel area of the Montaguto landslide.

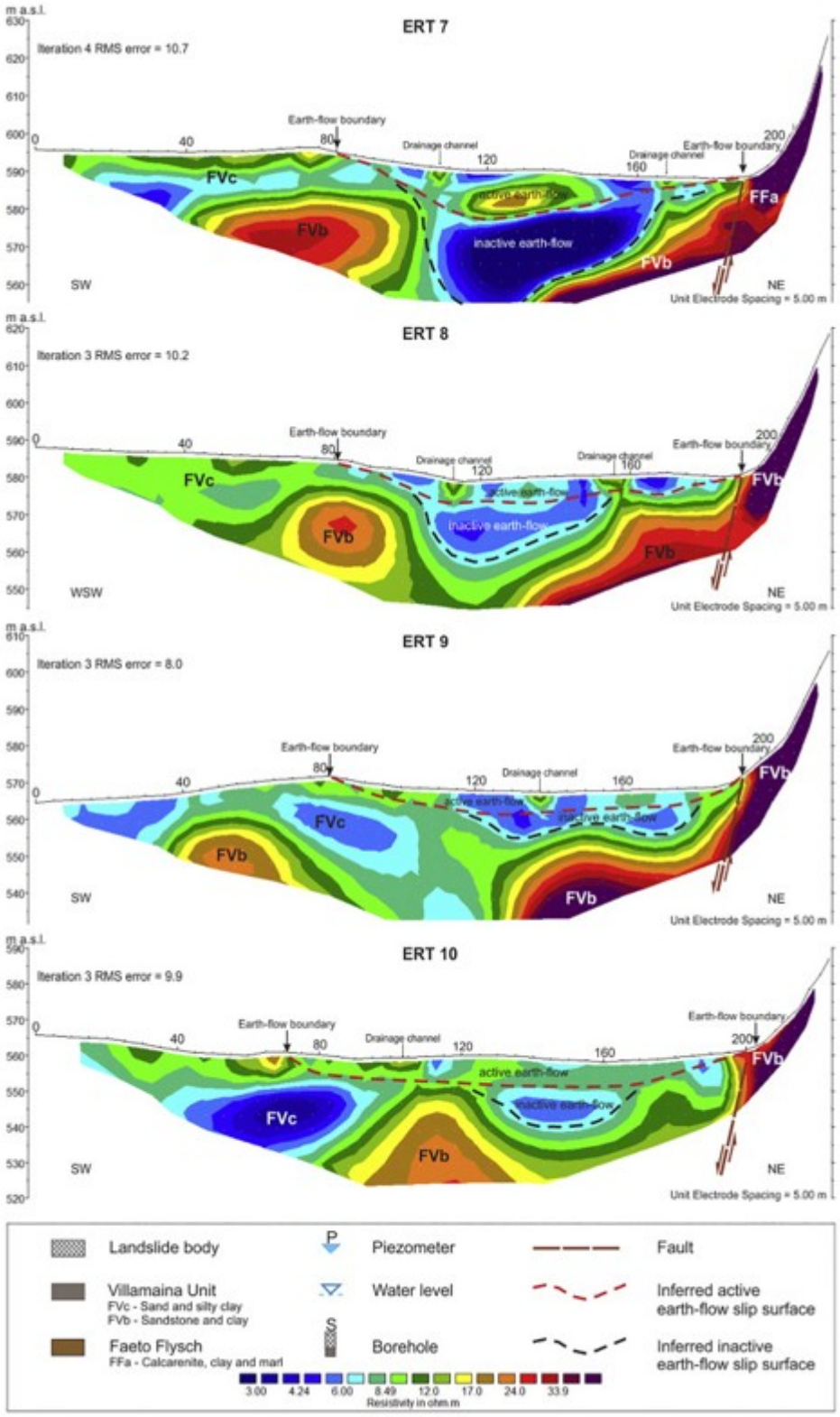

Fig. 5. Resistivity models of 7–10 ERT carried out in the central part of the channel area of the Montaguto landslide.

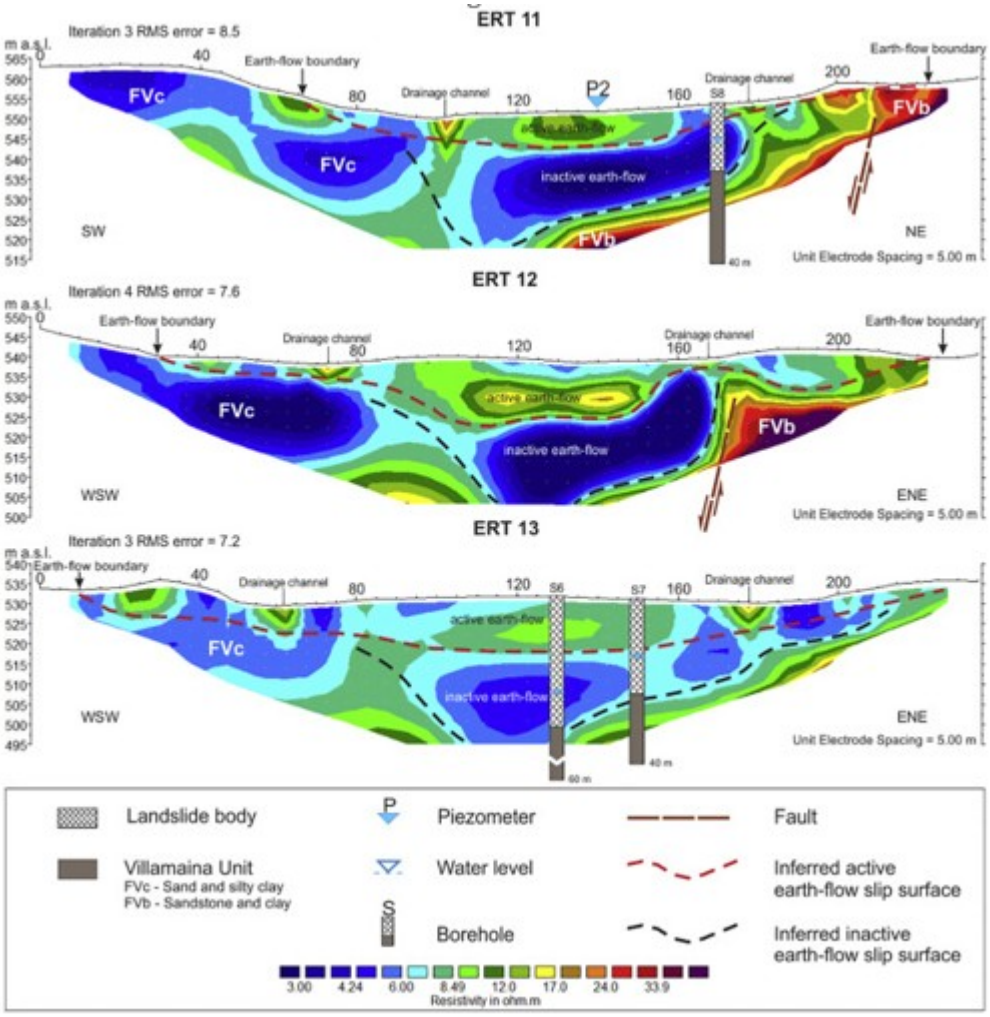

Fig. 6. Resistivity models of 11–13 ERT carried out in the central part of the channel area of the Montaguto landslide.

In particular, ERT 1 was placed parallel to one of the first drainage trenches, installed in the investigated area at an elevation of about 700 m a.s.l., and shows both vertical and horizontal resistivity variations. Between 85 and 180 m a relatively resistive superficial sector ($8 < \rho < 25\ \Omega m$) of about 10–12 m thickness is clearly identifiable, which likely corresponds to the drainage trench and active landslide material. At the bottom, a relatively conductive layer ($\rho < 12\ \Omega m$), laterally limited by more resistive zones ($\rho > 12\ \Omega m$), could be associated with the clayey lithofacies (FFa). By comparing the ERT with geological information, the more resistive zone located in the SE portion could be related to the calcareous-marly lithofacies (FFa) and the sub-vertical resistivity discontinuity could be due to the presence of a NE-SW normal fault, as reported in the map of Fig. 2, according to Guerriero et al. (2014). In the NW part of the image, the deep more resistive zone can be associated with FFa. Finally, the shallow lenticular low resistivity zone in the NW sector can be interpreted as FFa clayey facies.

ERT 2 was carried out between 625 and 650 m a.s.l. It is characterized by two shallow areas of conductive material ($\rho < 12\,\Omega$m) with lenticular shape, overlying a relatively resistive material ($\rho > 12\,\Omega$m). The first one, in the WSW sector of the image up to 100 m from the origin of the profile, may be associated with the inactive landslide body (IT in Fig. 2). The second one, in the central portion of the profile between 105 m and 170 m and with a maximum thickness of 10 m, is related to the active landslide. The more resistive material in the deeper part of the image, and the conductive area located at the eastern part of the ERT and bounded by the NE-SW normal fault, can be associated, respectively, with the calcareous and clayey facies of FFa.

All the electrical images realized in the central part of the channel area show similar resistivity patterns: the central part is characterized by conductive material of lenticular shape, confined within more resistive material by means of sub-vertical contacts. Only ERT 13 shows a different resistivity distribution, probably because it was located entirely inside the landslide body.

All the estimated resistivity models highlight the presence of the drainage channels that show up as very shallow resistive nuclei. Shallow moderate resistive material ($6 < \rho < 20\,\Omega$m) between drainage channels visible in all the ERT, except for ERT 9, can be associated with drained active landslide material reaching a maximum depth of about 15 m, according to Guerriero et al. (2014) and Lollino et al. (2014). Conductive material ($\rho < 6$–$7\,\Omega$m), characterizing the central and deep part of the ERT images, can be associated with the presence of higher water content than the surrounding material. This assumption is supported by the measured water tables at boreholes S6, S7, and S8, and by the pore water pressures recorded at the P1 and P2 piezometers (Lollino et al., 2014). The lenticular shape of this material could also be related to an old inactive landslide body, located below the currently active one, reaching a maximum thickness of about 30 m. This old landslide material seems to be confined in a paleo-channel characterized by relatively resistive boundaries. The more resistive material in the deeper part of ERT image could be related to FFa (ERT 3 to ERT 6) or to FVb (ERT 7 to ERT 11).

The NE part of almost all ERT images is characterized by high electrical resistivity values that are associated with material not affected by the movement and belonging to FFa (ERT 3 to ERT 7) and to FVb (ERT 8 to ERT 12). Conductive material visible at the end of profiles ERT 1 - ERT 4 could be related to FFa. The sub-vertical resistivity discontinuities in the NE sector of all ERT profiles (except for ERT 13) could be associated with the extension of the NE-SW normal fault, partially reported in Fig. 3 in Guerriero et al. (2014). The SW portions of all profiles consist of low-medium resistive material related to a sandy formation with silty clay beds (FVc). In addition, Fig. 7 shows a fence diagram showing the locations of the 2D ERT models (from

ERT 3 to ERT 13) in a perspective view within 3D space, highlighting the spatial consistency of the described features.

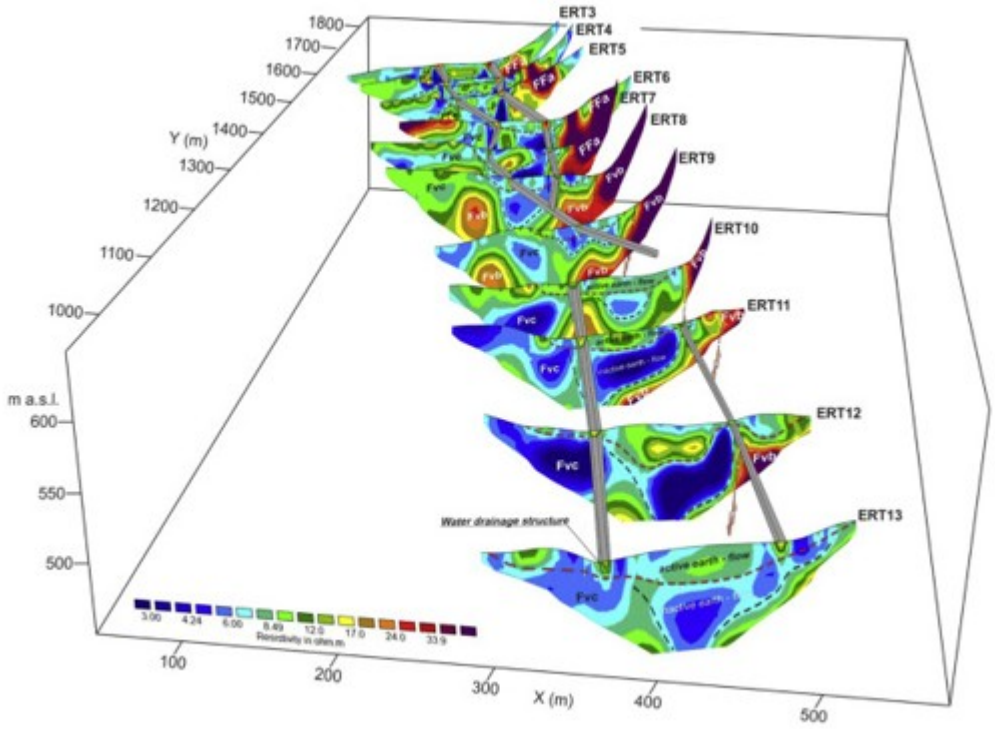

Fig. 7. Fence diagram showing the locations of the 2D ERT (ERT 3 – ERT 13) within a 3D space.

5. Conclusions

This paper reports the results of geoelectrical surveys carried out on the Montaguto landslide in order to improve the geometrical characterization of the landslide body and the definition of the geological setting. In particular, the survey was focused on a sector of the landslide channel, between about 600 and 520 m a.s.l., where continuous movements were evident, despite recent drainage interventions.

Although electrical resistivity contrasts in the ERT images were not very pronounced, it was possible to observe the presence of both lateral and vertical discontinuities, which can be ascribed to lithological boundaries and/or physical variations of the same material with varying water content. Regarding the geometrical characterization of landslide body and the reconstruction of the geological setting in the channel area, the resistivity distribution in ERT images has highlighted the following features:

- the active landslide material, due to the 2010 reactivation and reaching a maximum thickness of 15 m, is characterized by low-medium resistivity values ($6 < \rho < 20\ \Omega m$) and seems to be visible in almost all ERT images;

- the inactive earth-flow, characterized by prevalently very low resistivity values ($\rho < 6–7\ \Omega m$) and a well-defined lenticular shape with a maximum

thickness of about 25–30 m, is clearly visible in the ERT sections obtained in the central part of the channel area;

- lateral resistivity discontinuities, especially characterizing the NE sector of the central part of the channel area, represent the lateral limits of both the active and inactive landslide body. In some cases, these lateral limits are sub-vertical and can be associated with the presence of tectonic structures (normal fault), according to the morphology of the slope and previous geological studies carried out in the area (Guerriero et al., 2014). In contrast, in the SW portion the superficial lateral limits of the landslide body do not seem to be marked by clear resistivity contrasts due to the similar nature of the outcropping lithotypes (FVc: sand and silty clay).

Furthermore, the ERT surveys allowed the identification of the drainage channels built in the middle sector of landslide body. These structures are located in the uppermost shallow layers of the subsoil and are characterized by comparably high resistivity values ($\rho > 12\,\Omega m$). From a geophysical point of view, considering that the material included between the drainage channels is characterized by moderately resistivity values ($6 < \rho < 20\,\Omega m$) in comparison to the more conductive surrounding material, it is possible to hypothesize that the complex drainage system installed on the slope is effective in continuously draining and drying the subsoil. It is worth noting that only a multi-temporal survey (e.g. by using time-lapse ERT and in situ pore pressure measurements) could verify the effectiveness of this intervention.

The identification of high water content areas, supported by the measured water tables at some boreholes, could be taken into account in the designing of additional drainage systems.

The results obtained by the geoelectrical surveys could be considered for the planning of more appropriate actions aimed at the stabilization of the investigated sector of the Montaguto landslide by the Italian National Civil Department.

Acknowledgements

This work was partially funded by the National Department of Civil Protection (DPC) (rep. N.1177 on 10/12/12). We thank the researchers of CNR-IRPI for providing data used for the calibration and interpretation of geoelectrical survey.

References

Amore et al., 1998

O. Amore, C. Basso, G. Ciampo, S. Ciarcia, V. Di Donato, S. Di Nocera, P. Esposito, F.Matano, D. Staiti, M. Torre**Nuovi dati stratigrafici sul Pliocene affiorante tra il fiume Ufita ed il torrente Cervaro (Irpinia, Appennino meridionale)**

Boll. Soc. Geol. Ital., 117 (1998), pp. 455-466

(in Italian)

Calamita et al., 2017

G. Calamita, A. Perrone, L. Brocca, S. Straface**Soil electrical resistivity for spatial sampling design, prediction, and uncertainty modeling of soil moisture**

Vadose Zone J., 16 (10) (2017)

Centro funzionale multirischi della Regione Campania, n.d

Centro funzionale multirischi della Regione Campania

http://centrofunzionale.regione.campania.it/#/pages/sensori/archivio-pluviometrici

Chambers et al., 2011

J.E. Chambers, P.B. Wilkinson, O. Kuras, J.R. Ford, D.A. Gunn, P.I. Meldrum, C.V.L.Pennington, A.L. Weller, P.R.N. Hobbs, R.D. Ogilvy**Three-dimensional geophysical anatomy of an active landslide in Lias Group mudrocks, Cleveland Basin, UK**

Geomorphology, 125 (2011), pp. 472-484

Crostella and Vezzani, 1964

A. Crostella, L. Vezzani**La geologia dell'Appennino Foggiano**

Boll. Soc. Geol. Ital., 83 (1964), pp. 121-141

(in Italian)

Cruden and Varnes, 1996

D.M. Cruden, D.J. Varnes**Landslide types and processes**

A.K. Turner, R.L. Schuster (Eds.), Landslides, Investigation and Mitigation, Special Report 247, Transportation Research Board, Washington D.C. (1996), pp. 36-75

(ISSN: 0360-859X ISBN: 030906208X)

Dazzaro et al., 1988

L. Dazzaro, S. Di Nocera, T. Pescatore, L. Rapisardi, M. Romeo, B. Russo, M.R. Senatore, M. Torre**Geologia del margine della Catena Appenninica tra il F. Fortore ed il T. Calaggio (Monti della Daunia – Appennino Meridionale)**

Mem. Soc. Geol. Ital., 41 (1988), pp. 411-422

(in Italian)

Desiato et al., 2007

F. Desiato, F. Lena, A. Toreti**SCIA: a system for a better knowledge of the Italian climate**

Boll. Geofis. Teor. Appl., 48 (3) (2007), pp. 351-358

Di Nocera and Torre, 1987

S. Di Nocera, M. Torre**Geologia dell'area compresa tra Deliceto e Scampitella (Appennino Foggiano)**

Boll. Soc. Geol. Ital., 106 (1987), pp. 351-364

(in Italian)

Di Nocera et al., 2011

S. Di Nocera, F. Matano, T. Pescatore, F. Pinto, M. Torre**Caratteri geologici del settore esterno dell'Appennino campano-lucano nei Fogli CARG**

Rend. Online Soc. Geol. Ital., 12 (2011), pp. 39-43

(in Italian)

Ferrigno et al., 2017

F. Ferrigno, G. Gigli, R. Fanti, E. Intrieri, N. Casagli**GB-InSAR monitoring and observational method for landslide emergency management: the Montaguto earthflow (AV, Italy)**

Nat. Hazards Earth Syst. Sci., 17 (2017), pp. 845-860

Gallipoli et al., 2000

M.R. Gallipoli, V. Lapenna, P. Lorenzo, M. Mucciarelli, A. Perrone, S. Piscitelli, F. Sdao**Comparison of geological and geophysical prospecting techniques in the study of a landslide in southern Italy**

Eur. J. Environ. Eng. Geophys., 4 (2000), pp. 117-128

Giocoli et al., 2008

Giocoli, A., Magrì, C., Piscitelli, S., Rizzo, E., Siniscalchi, A., Burrato, P., Vannoli, P., Basso, C., Di Nocera, S., 2008. Electrical resistivity tomography investigations in the Ufita Valley (southern Italy), Ann. Geophys.-Italy, 51, 213–223.

Giocoli et al., 2015

A. Giocoli, T.A. Stabile, I. Adurno, A. Perrone, M.R. Gallipoli, E. Gueguen, E. Norelli, S.Piscitelli**Geological and geophysical characterization of the southeastern side of the High Agri Valley (southern Apennines, Italy)**

Nat. Hazards Earth Syst., 15 (2015), pp. 315-323, 10.5194/nhess-15-315-2015

Giordan et al., 2013

D. Giordan, P. Allasia, A. Manconi, M. Baldo, M. Santangelo, M. Cardinali, A. Corazza, V.Albanese, G. Lollino, F. Guzzetti**Morphological and kinematic**

evolution of a large earthflow: the Montaguto landslide, southern Italy

Geomorphology, 187 (2013), pp. 61-79, 10.1016/j.geomorph.2012.12.035

Guerriero et al., 2013

L. Guerriero, P. Revellino, J.A. Coe, M. Focareta, G. Grelle, V. Albanese, A. Corazza, F.M.Guadagno**Multi-temporal maps of the Montaguto earth flow in southern Italy from 1954 to 2010**

J. Maps, 9 (1) (2013), pp. 135-145, 10.1080/17445647.2013.765812

Guerriero et al., 2014

L. Guerriero, J.A. Coe, P. Revellino, G. Grelle, F. Pinto, F.M. Guadagno**Influence of slip-surface geometry on earth-flow deformation, Montaguto earth flow, southern Italy**

Geomorphology, 219 (2014), pp. 285-305, 10.1016/j.geomorph.2014.04.039

Guzzetti, 2006

F. Guzzetti**Landslide Hazard and Risk Assessment**

Universitäts-und Landesbibliothek Bonn (2006)

PhD Thesis

Hack, 2000

R. Hack**Geophysics for slope stability**

Surv. Geophys., 21 (2000), pp. 423-448

Jongmans and Garambois, 2007

D. Jongmans, S. Garambois**Geophysical investigation of landslides: a review**

Bull. Soc. Geol. Fr., 178 (2) (2007), pp. 101-112, 10.2113/gssgfbull.178.2.101

Lapenna et al., 2003

V. Lapenna, P. Lorenzo, A. Perrone, S. Piscitelli, E. Rizzo, F. Sdao**High-resolution geoelectrical tomographies in the study of the Giarrossa landslide (Potenza, Basilicata)**

Bull. Eng. Geol. Environ., 62 (2003), pp. 259-268

Lapenna et al., 2005

V. Lapenna, P. Lorenzo, A. Perrone, S. Piscitelli, E. Rizzo, F. Sdao**2D electrical resistivity imaging of some complex landslides in Lucanian Apennine chain, southern Italy**

Geophysics, 70 (3) (2005), pp. B11-B18

Lebourg et al., 2005

T. Lebourg, S. Binet, E. Tric, H. Jomard, S. El Bedoui**Geophysical survey to estimate the 3D sliding surface and the 4D evolution of the water pressure on part of a deep-seated landslide**

Terra Nova, 17 (2005), pp. 399-406, 10.1111/j.1365-3121.2005.00623.x

Loke, 2004

M.H. Loke**Tutorial: 2-D and 3-D Electrical Imaging Surveys**

Geotomo Software, Malaysia (2004)

Available at:

http://www.geotomosoft.com

Loke and Barker, 1996

M.H. Loke, R.D. Barker**Rapid least-squares inversion of apparent resistivity pseudosections by a quasi-newton method**

Geophys. Prospect., 44 (1996), pp. 131-152

Lollino et al., 2013

G. Lollino, P. Allasia, D. Giordan, F. Guzzetti, P. Lollino, M. Baldo**Studio della frana di Montaguto (AV) con tecniche di monitoraggio integrato. BURC N.1 07/01/2014**

Allegato Tecnico (2013), pp. 1-14

http://burc.regione.campania.it/eBurcWeb/publicContent/archivio/archivio.iface

(in Italian)

Lollino et al., 2014

P. Lollino, D. Giordan, P. Allasia**The Montaguto earthflow: a back-analysis of the process of landslide propagation**

Eng. Geol., 170 (2014), pp. 66-79, 10.1016/j.enggeo.2013.12.011

McCann and Forster, 1990

D.M. McCann, A. Forster**Reconnaissance geophysical methods in landslide investigations**

Eng. Geol., 29 (1990), pp. 59-78

Mucciarelli et al., 2009

M. Mucciarelli, G. Böhm, R. Caputo, A. Giocoli, E. Gueguen, P. Klin, L. Marello, F.Palmieri, S. Piscitelli, E. Priolo, G. Romano, E. Rizzo**Caratteri geologici e geofisici dell'area di San Giuliano di Puglia**

Riv. Ital. Geotecnica, 3 (2009), pp. 32-42

Naudet et al., 2008

V. Naudet, M. Lazzari, A. Perrone, A. Loperte, S. Piscitelli, V. Lapenna**Integrated geophysical and geomorphological approach to investigate the snowmelt-triggered landslide of Bosco Piccolo village (Basilicata, southern Italy)**

Eng. Geol., 98 (2008), pp. 156-167

Niesner and Weidinger, 2008

E. Niesner, J.T. Weidinger**Investigation of a historic and recent landslide area in ultrahelvetic sediments at the northern boundary of the Alps (Austria) by ERT measurements**

Lead. Edge, 27 (11) (2008), pp. 1498-1509

Perrone et al., 2004

A. Perrone, A. Iannuzzi, V. Lapenna, P. Lorenzo, S. Piscitelli, E. Rizzo, F. Sdao**High-resolution electrical imaging of the Varco d'Izzo earthflow (southern Italy)**

J. Appl. Geophys., 56 (2004), pp. 17-29

Perrone et al., 2006

A. Perrone, G. Zeni, S. Piscitelli, A. Pepe, A. Loperte, V. Lapenna, R. Lanari**Joint analysis of SAR interferometry and electrical resistivity tomography surveys for investigating ground deformation: the case-study of Satriano di Lucania (Potenza, Italy)**

Eng. Geol., 88 (2006), pp. 260-273

Perrone et al., 2014

A. Perrone, V. Lapenna, S. Piscitelli**Electrical resitivity tomography technique for landslide investigation: a review**

Earth Sci. Rev., 135 (2014), pp. 65-82, 10.1016/j.earscirev.2014.04.002

Pescatore et al., 1996

T. Pescatore, B. Russo, M.R. Senatore, G. Ciampo, P. Esposito, F. Pinto, D. Staiti**La successione messiniana della valle del Torrente Cervaro (Appennino Dauno, Italia Meridionale)**

Boll. Soc. Geol. Ital., 115 (1996), pp. 369-378

(in Italian)

Robert et al., 2011

T. Robert, A. Dassargues, S. Brouyère, O. Kaufmann, V. Hallet, F. Nguyen**Assessing the contribution of electrical resistivity tomography (ERT) and self-potential (SP) methods for a water well drilling program in fractured/karstified limestones**

J. Appl. Geophys., 75 (1) (2011), pp. 42-53, 10.1016/j.jappgeo.2011.06.008

Santo and Senatore, 1988

A. Santo, M.R. Senatore**La successione stratigrafica dell'Unità Dauna a Monte Sidone (Castelluccio Valmaggiore - Foggia)**

Mem. Soc. Geol. Ital., 41 (1988), pp. 431-438

(in Italian)

Sasaki, 1992

Y. Sasaki**Resolution of resistivity tomography inferred from numerical simulation**

Geophys. Prospect., 40 (1992), pp. 453-463

Sharma and Verma, 2015

S. Sharma, G.K. Verma**Inversion of electrical resistivity data: a review**

World Academy of Science, Engineering and Technology

Int. J. Environ. Chem. Ecol. Geol. Geophys. Eng., 9 (4) (2015), pp. 400-406

Supper et al., 2013

R. Supper, I. Baro, D. Ottowitz, K. Motschka, S. Gruber, E. Winkler, B. Jochum, A. Römer**Airborne geophysical mapping as an innovative methodology for landslide investigation: evaluation of results from the Gschliefgraben landslide, Austria**

Nat. Hazards Earth Syst. Sci., 13 (2013), pp. 3313-3328, 10.5194/nhess-13-3313-2013

Uhlemann et al., 2017

S. Uhlemann, J. Chambers, P. Wilkinson, H. Maurer, A. Merritt, P. Meldrum, O. Kuras, D.Gunn, A. Smith, T. Dijkstra**Four-dimensional imaging of moisture dynamics during landslide reactivation**

J. Geophys. Res. Earth Surf., 122 (2017), pp. 398-418, 10.1002/2016JF003983

Ventura et al., 2011

G. Ventura, G. Vilardo, C. Terranova, E. Bellucci Sessa**Tracking and evolution of complex active landslides by multi-temporal airborne LiDAR data: the Montaguto landslide (Southern Italy)**

Remote Sens. Environ., 115 (12) (2011), pp. 3237-3248

[1] Now at: Department of Geophysics, Lawrence Berkeley National Laboratory, Berkeley, USA.